Toxicology Letters 198 (2010) 237–243

Contents lists available at ScienceDirect

Toxicology Letters

journal homepage: www.elsevier.com/locate/toxlet

Biodistribution and toxicity of nanodiamonds in mice after intratracheal instillation

Xiaoyong Zhang[a,b], Jilei Yin[a,c], Cheng Kang[a], Jing Li[a,b], Ying Zhu[a], Wenxin Li[a,*], Qing Huang[a,*], Zhiyong Zhu[a,*]

[a] Laboratory of Physical Biology, Shanghai Institute of Applied Physics, Chinese Academy of Sciences, 2019 Jialuo Road, Jiading, Shanghai 201800, China
[b] Graduate School of Chinese Academy of Sciences, Beijing 100049, China
[c] TCM Branch of Jiangsu Union Technical Institute, Lianyungang 222006, China

ARTICLE INFO

Article history:
Received 4 January 2010
Received in revised form 28 June 2010
Accepted 1 July 2010
Available online 13 July 2010

Keywords:
Nanodiamonds
Biodistribution
Micro-SPECT
Intratracheal instillation
Toxicity

ABSTRACT

Nanodiamonds (NDs) are receiving increasing attention in materials science and nanotechnology-based industries for a large variety of applications, including protein immobilization, biosensors, therapeutic molecule delivery, and bioimaging. However, limited information is known about their biokinetic behavior and toxicity *in vivo*. In this article, we investigated the biodistribution of NDs using radiotracer techniques and evaluated its acute toxicity in Kun Ming mice after intratracheal instillation. The biodistribution showed that, besides having the highest retention in the lung, NDs were distributed mainly in the spleen, liver, bone and heart. An analysis of histological morphology and biochemical parameters indicated that NDs could induce dose-dependent toxicity to the lung, liver, kidney and blood. This work provided fundamental data for understanding the biodistribution of NDs and will provide guidance for further study of their toxicity.

1. Introduction

With the development of nanoscience and nanotechnology, carbon nanomaterials have received much attention in materials science and nanotechnology-based industries (Thostenson et al., 2001). A large variety of applications for carbon nanomaterials have been proposed, including catalysis, electronic devices, and drug delivery vehicles (Sun et al., 2002). As the applications and industrial production of these nanomaterials become more widespread, there will inevitably be an increase in the potential risk to humans from exposure, and raise additional concerns about their short- and long-term toxicological effects (Lam et al., 2006). The toxicology of carbon nanotubes and C_{60} has recently become an area of intensive investigation (Bottini et al., 2006; Donaldson et al., 2006; Magrez et al., 2006; Ueng et al., 1997), however, other engineered carbon nanomaterials, such as NDs and graphene oxide have not received as much attention.

NDs are a relatively new class of carbon nanomaterials that possess a diamond structure at the nanometer scale. As with carbon nanotubes and fullerenes, NDs are beginning to emerge as alternative candidates for biomedical applications (Boudou et al., 2009; Chen et al., 2009) due to their optical transparency, chemical inertness, high specific area, and hardness. It has been suggested that NDs may prove to be an even better drug carrier (Huang et al., 2007), imaging probe (Chao et al., 2007; Fu et al., 2007), or implant coating (Huang et al., 2008) in biological systems compared with other carbon nanomaterials. To date, however, only limited information is known about their biological behavior *in vivo* and their toxicological effects to the environment and the human body (Puzyr et al., 2007; Yuan et al., 2009).

Previous work has demonstrated that NDs show little toxicity to a variety of cell types and do not produce significant reactive oxygen species (Liu et al., 2007a; Schrand et al., 2007a; Yu et al., 2005). Furthermore, recent studies on carbon nanomaterials for biological applications have revealed that NDs are much more biocompatible than most of other carbon nanomaterials (Schrand et al., 2007b). The work of Puzyr et al. (2007) showed that no indications of inflammatory processes were found after 3 months of subcutaneous exposure to NDs in mice, however, when studied in rabbits, a number of blood biochemical parameters were affected after intravenous administration of NDs, suggesting that exposure routes could influence the toxicity effects of NDs observed in animals. It is well known that the human body may be exposed to nanoparticles through four routes: inhalation of airborne nanoparticles, ingestion of drinking water or food additives, dermal penetration by skin contact, and injection of engineered nanomaterials. Although previous studies have indicated that NDs were biocompatible with rats and

* Corresponding authors. Tel.: +86 21 39194530; fax: +86 21 59553021.
E-mail addresses: liwenxin@sinap.ac.cn (W. Li), qhuang1974@sinap.ac.cn (Q. Huang), zhuzhiyong@sinap.ac.cn (Z. Zhu).

0378-4274/$ – see front matter.
doi:10.1016/j.toxlet.2010.07.001

mice after intraperitoneal injection and subcutaneous exposure, thus far, no studies have focused on the biodistribution and toxicity of NDs after inhalation by test animals of airborne nanoparticles.

Intratracheal instillation has become a widely applied technique for the investigation of the respiration toxicity of nanoparticles due to its simplicity and reproducibility. In this work, the biodistribution and toxicity of NDs in Kun Ming mice were investigated by intratracheal instillation. The results of the investigation demonstrated that NDs were mainly accumulated in the lung. A fraction of the NDs were transported into the blood via the air–blood barrier, and then redistributed in the liver, spleen, bone and heart. Besides inducing significant toxicity to the lungs, other organs including the liver, kidney and the hematological system were adversely influenced after intratracheal instillation of NDs. These results provided fundamental information on both the biodistribution and respiratory toxicity of NDs after intratracheal instillation in mice, allowing for a better understanding of the risk that NDs pose to human health via respiratory exposure.

2. Materials and methods

2.1. Materials and reagents

NDs with individual sizes ranging from 2 to 10 nm, generously supplied by Gansu Gold Stone Nano.Material Co., Ltd., were synthesized by detonation techniques. As-received NDs were characterized by a series of spectroscopy techniques and analytical methods. Fourier transform-infrared spectroscopy (FT-IR, Nicolet Avatar-360) showed that the NDs were functionalized with –OH and –COOH on the surface. Thermogravimetric analysis (TGA, PerkinElmer, USA) indicated that the weight of functionalized groups amounted to 1.9%. On the bases of measurements with inductively coupled plasma mass spectrometry (ICP-MS, X-7, Thermo-elemental, USA), we ascertained that the main impurities in NDs were Fe (0.1%), Al (0.1%), and Ba, Mn, and Ni (0.001% for each), and the purity of the NDs was estimated to be over 95%. The scanning electron microscopy (SEM, LEO-1530VP, Germany) showed that the sizes of majority of ND aggregates were about 40–100 nm (Fig. 1). The detailed data of characterization will be described elsewhere. As-received NDs were used directly to the experiments without any pretreatment. All of the other reagents used in this study were of at least analytical grade.

2.2. Animals

Kun Ming mice (male 20 ± 2 g, 6–8 weeks) were purchased from Shanghai SLAC Laboratory Animal Co. Ltd., China. The mice were checked for the absence of infection for 1 week prior to experimentation. The mice were housed in plastic cages, fed a commercial diet, and given water *ad libitum*. Permission of the local ethics committee was obtained, and all animal experiments were performed according to Chinese law and accepted international standards in biomedical research.

2.3. Synthesis and stability of ^{188}Re-NDs

$Na^{188}ReO_4$ in normal saline was obtained from an alumina-based $^{188}W/^{188}Re$ radionuclide generator (Shanghai Ke Xing Pharmaceutical Co). The ^{188}Re-NDs were synthesized by a general method. In brief, 1 mL of NDs (1 mg/mL), 50 μL ascorbic acid (40 mg/mL), 70 μL stannous chlorides (60 mg/mL) and 1 mCi $Na^{188}ReO_4$ were reacted in water bath at 80 °C for 25 min. The unreacted $Na^{188}ReO_4$ was removed by applying a normal saline wash three times. The labeled compound was then dispersed with phosphate buffer saline (PBS) before the biodistribution experiment.

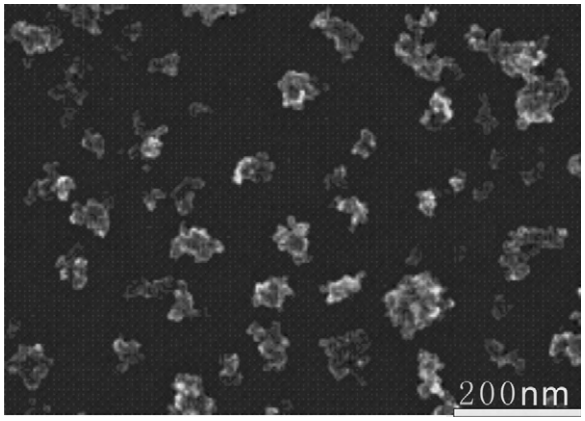

Fig. 1. Scanning electron microscopy (SEM) images of NDs, scale bar 200 nm.

Radiolabeling yields of ^{188}Re-NDs were determined by paper chromatography (PC) using Whatman 1 paper strips. 10 μL portions of the test solution were applied at 1.5 cm from the lower end of the strips. The strips were developed in normal saline until the solvent reached the top portion. The strips were dried and cut into 1 cm long equal segments, and the radioactivity was measured by using a Gamma-ray counter. Retardation factors of $Na^{188}ReO_4$ and ^{188}Re-NDs were 0.9–1 and 0, respectively.

To determine the stability of ^{188}Re-NDs *in vitro*, a purified labeling compound was incubated with a RPMI-1640 cell culture medium with 10% fetal bovine serum (FBS) at 37 °C for 48 h. Drops of NDs-serum or suspension were collected at different time points and examined for radiochemical purity by PC as described previously. Variations in the radiochemical purity over different time intervals showed the *in vitro* stability of the ^{188}Re-NDs.

To examine the stability of ^{188}Re-NDs *in vivo*, mice were randomly divided into two groups. 50 μCi of ^{188}Re-NDs was administered to mice by intratracheal instillation. Then, blood samples were taken from the orbital vein of each mouse at 4 h post-intratracheal instillation and were anticoagulated and centrifuged at 14,000 rpm for 5 min. The radioactivity present in the supernatant and sediment was measured by a gamma-ray counter, so that the radiochemical purity of the labeling compounds in blood could be established. In control experiments, about 50 μCi of $Na^{188}ReO_4$ was administered to mice by intratracheal instillation. The blood samples were taken at 1 h and 4 h post-administration. After centrifuged at 14,000 rpm for 5 min, the activities present in the supernatant and sediment were determined for correction of the data on *in vivo* stability of ^{188}Re-NDs.

2.4. Biodistribution of ^{188}Re-NDs after intratracheal instillation

A biodistribution study was performed with 40 Kun Ming mice (male), which were randomly divided into five groups. Mice were anesthetized with pentobarbital sodium and 20 μCi ^{188}Re-NDs were administrated to each mouse by intratracheal instillation. At different time points, the mice were sacrificed by dislocation of the vertebrae, and important organs and tissues were excised, weighed, and measured with a gamma-ray counter. The uptake of the radiolabeled NDs in different organs and tissues was expressed as the percentage of the injected dose per gram of tissue (% ID/g), as shown in Eq. (1). The resultant data were expressed as mean values with the standard deviation:

$$\text{Organ uptake} = \frac{\text{Organ radioactivity}}{\text{Total radioactivity} \times \text{organ weight (g)}} \times 100\% \quad (1)$$

2.5. Acute toxicity of NDs exposure by intratracheal instillation

2.5.1. General experimental design

Kun Ming mice were randomly divided into five groups: control group, PBS group and three experimental groups (0.8 mg/kg, 4 mg/kg, and 20 mg/kg body weight). Mice were anesthetized with pentobarbital sodium and then either a 0.2 mL PBS or NDs suspension was administrated by intratracheal instillation, with the untreated mice serving as a control. To assess the acute toxicity of NDs, several toxicity features were investigated at 3 days post-exposure, including: (1) histopathology of lung tissue, (2) biochemical parameters of bronchoalveolar lavage fluids (BAL fluids), (3) biochemical parameters of blood, and (4) complete blood cell counts.

2.5.2. Histopathological morphology studies

For pathological studies, all histopathological tests were performed using standard laboratory procedures. The tissues were embedded in paraffin blocks, then sliced into 5 μm thick sections and placed onto glass slides. After hematoxylin–eosin staining, the slides were observed and photographs were taken using an optical microscope (Motorized inverted system microscope IX81/IX81-ZDC, Japan). The pathologist performing the visual analysis was blinded to the sample identifier and results of the other histopathological analyses.

2.5.3. Bronchoalveolar lavage fluids

The lungs of the control group, PBS group and NDs-exposed mice were lavaged with a warmed PBS solution as described previously (Li et al., 2007a). In brief, the first 4 mL of lavaged fluids recovered from the lungs of the PBS group or NDs-exposed mice was centrifuged at $700 \times g$, and 2 mL of the supernatant was removed for biochemical parameter studies. All of the biochemical assays were performed on a BAL analyzer using a Roche Diagnostics (BMC)/Hitachi 7080 clinical chemistry analyzer and Roche Diagnostics (BMC)/Hitachi reagents. Lactate dehydrogenase (LDH), malondialdehyde (MDA) and lavage fluid protein were identified using the Roche Diagnostics (BMC)/Hitachi reagents.

2.5.4. Blood biochemical parameter analyses

In the present study, liver function was evaluated by measuring serum levels of alanine aminotransferase (ALT), aspartate aminotransferase (AST), and alkaline phosphatase (ALP). Nephrotoxicity was determined by measuring blood urea nitrogen (BUN) and creatinine (Cr).

Table 1
Biodistribution of ^{188}Re-NDs in Kun Ming mice (%ID/g, mean ± SD) (n = 8).

Organ	Time after intratracheal instillation				
	1 h	4 h	10 h	24 h	48 h
Heart	1.80 ± 0.22	0.77 ± 0.08	0.77 ± 0.10	0.52 ± 0.10	0.52 ± 0.11
Liver	0.52 ± 0.05	0.62 ± 0.08	0.94 ± 0.07	0.35 ± 0.08	0.30 ± 0.10
Spleen	1.96 ± 0.20	1.48 ± 0.15	1.03 ± 0.12	0.80 ± 0.08	1.16 ± 0.08
Lung	192.3 ± 42.24	186.4 ± 32.99	125.21 ± 34.15	90.7 ± 32.86	69.1 ± 14.5
Kidney	0.60 ± 0.11	0.74 ± 0.13	1.46 ± 0.26	0.58 ± 0.11	0.49 ± 0.11
Brain	0.30 ± 0.10	0.33 ± 0.11	0.30 ± 0.11	0.20 ± 0.08	0.38 ± 0.10
Bone	1.21 ± 0.16	1.10 ± 0.13	1.42 ± 0.11	1.01 ± 0.13	1.69 ± 0.15
Urine	1.00 ± 0.10	1.42 ± 0.30	2.75 ± 0.55	4.64 ± 0.50	0.26 ± 0.05
Blood	1.00 ± 0.10	0.63 ± 0.07	0.40 ± 0.05	0.26 ± 0.03	0.19 ± 0.02
Stomach	0.38 ± 0.05	0.20 ± 0.37	0.54 ± 0.58	0.43 ± 0.15	0.38 ± 0.10

2.5.5. Complete blood counts

For complete blood counts (CBC), 75 μL of blood was collected by retro-orbital bleed at 3 days post-exposure through a heparin-coated glass capillary. CBC and chemistry panel determinations were performed by using an Automated Hematology Analyzer (Advia 120, Bayer, Germany) at Shanghai University of Traditional Chinese Medicine (Drug Safety Evaluation Center).

2.5.6. Statistical analyses

For the analysis, each of the experimental values was compared to their corresponding PBS control value. A one-way ANOVA test and Bartlett's test were calculated for each sampling time. When the F-test from ANOVA was significant, the Dunnett test was used to compare means from the control group and each of the groups exposed to particulates. Significance was judged at the 0.05 and 0.01 probability level.

3. Results

3.1. The stability of ^{188}Re-NDs

Measurements made by PC showed that the radiolabeling yields of ^{188}Re-NDs were greater than 93% (data not shown). According to the amounts of chemicals used in labeling reaction, the ratio of Re atoms to ND was estimated roughly to be as low as 10^{-6}. After purification, the radiochemical purity of ^{188}Re-NDs increased to 98.5%. And after incubation with FBS for 48 h, the radiochemical purity of ^{188}Re-NDs amounted to 92%, confirming the excellent stability of ^{188}Re-NDs *in vitro*. The study of *in vivo* stability indicated that 86% activity in the blood samples, mainly ^{188}Re-NDs, was settled down in the sediment after centrifugation. As showed in the control experiments, a part of $Na^{188}ReO_4$ in blood samples would be also settled down in the sediment. After correction for the contribution of free $Na^{188}ReO_4$, the radiochemical purity of ^{188}Re-NDs in blood maintained a fairly good level of approximately 80% at 4 h post-exposure.

3.2. Biodistribution of NDs after intratracheal instillation

The data describing the biodistribution of ^{188}Re-NDs in mice after intratracheal instillation are presented in Table 1. It can be seen that the lung had the highest uptake; the values of % ID/g remained at approximately 190% within 4 h after intratracheal instillation. ^{188}Re-NDs could be transported into the blood circulation system, and then redistributed mainly into the spleen, bone, liver, and heart, with no uptake was found in the brain. Finally, the radioactivity was excreted in a form of $Na^{188}ReO_4$, as confirmed by PC during an investigation of radiochemical purity in a separate experiment.

3.3. Toxicity of NDs in vivo

3.3.1. Organ histopathological analysis

The toxicity assessments of NDs *in vivo* started at 3 days post-intratracheal instillation. The body and organ (liver, kidney and spleen) weights of the mice were determined; no obvious differences were found in body weight or coefficient of the liver, spleen, and kidney between the control group, the PBS group and the experimental groups. The histological sections of the lung, liver, kidney and spleen were examined, and no abnormal pathology changes in the liver, kidney, and spleen were found by photomicrography (not shown). On the contrary, as shown in Fig. 2, the histopathological analysis of lung tissues revealed that pulmonary exposure to NDs induced lung inflammatory responses characterized by neutrophils and foamy alveolar macrophage accumulation. Lung tissue thickening, as a prelude to the development of fibrosis, was evident and progressive. The significant lung toxicity of NDs observed (Fig. 2) was the result of a high retention of NDs in the lung, suggesting a dose-dependence of pulmonary toxicity.

Although NDs were well dispersed in PBS before instillation, as seen from Fig. 2, many clumps still existed in the bronchi and alveoli in the 4 mg/kg and 20 mg/kg groups. Apparently, these clumps formed from the aggregation of NDs that were too large to be phagocytized by the alveolar macrophages and consequently were not cleared in time. As a result, persistent pathological lesions would occur in the bronchi and alveoli.

3.3.2. Biochemical parameters in BAL fluids

In this work, a number of biochemical parameters in BAL fluids were measured to evaluate the toxicity of NDs to the lung. The measurements for the control group, PBS group and experimental groups are shown in Table 2. Total protein concentration in BAL fluids increased slightly with increasing exposure dose of NDs. A clear increase in total protein concentration was found in the 20 mg/kg group compared with the PBS group, suggesting that NDs exposure could induce the destruction of alveoli netted structures, thus enhancing the permeability of the lung. The production of MDA is a good indicator for the assessment of oxidative stress when living systems are exposed to xenobiotics. In this work, we found dose-dependent increases of MDA level in BAL fluids, while no distinct change of ALP level was found. The LDH activity in the BAL fluids increased significantly ($P < 0.05$) with NDs dose in all experimental groups. As can be seen from Table 2, LDH activity for the 20 mg/kg group increased by over 170% compared with the PBS group. The remarkable elevation of LDH activity reflected the damage to lung tissue induced by NDs.

3.3.3. Biochemical parameters in blood

To assess the systematic toxicity of NDs, a number of biochemical parameters in serum, such as ALT, AST, ALP, BUN, and Cr, were measured. Table 3 shows the changes in biochemical parameters in serum. It is well known that both ALT/AST ratios and ALP are biomarkers of liver damage. In our experiment, there were no significant changes in AST values after exposure to NDs particles. However, the ALT/AST ratios and ALP levels showed a

Table 2
Changes of biochemical parameters in the BAL fluids of mice induced by NDs ($n = 8$).

Groups	Protein (mg/mL)	MDA (μmol/L)	ALP (U/L)	LDH (U/L)
Control	0.20 ± 0.02	2.69 ± 0.21	1.19 ± 0.20	100 ± 8.02
PBS	0.48 ± 0.04	4.31 ± 0.34	1.29 ± 0.13	341.50 ± 15.08
0.8 mg/kg	0.514 ± 0.05	5.56 ± 0.41*	1.33 ± 0.15	414.34 ± 25.34**
4 mg/kg	0.52 ± 0.05	6.63 ± 0.43*	1.38 ± 0.17	524.012 ± 30.40**
20 mg/kg	0.54 ± 0.04*	7.64 ± 0.53*	1.30 ± 0.17	582.03 ± 30.53**

* A value significantly ($P < 0.05$) differed from the PBS group.
** A value significantly ($P < 0.01$) differed from the PBS group.

Table 3
Changes of biochemical parameters in the serum of mice induced by NDs ($n = 10$).

Groups	ALT	AST	ALT/AST	ALP	BUN	Cr
Control	34.40 ± 5.86	104.40 ± 18.44	0.33 ± 0.02	471.25 ± 31.61	6.03 ± 0.707	8.36 ± .047
PBS	34.06 ± 5.50	108.07 ± 21.41	0.32 ± 0.03	530.51 ± 45.96*	6.47 ± 1.15	8.43 ± 0.91
0.8 mg/kg	34.03 ± 7.07	101.50 ± 23.53	0.33 ± 0.03	665.52 ± 50.20**	6.64 ± 1.05	9.05 ± 1.06
4 mg/kg	37.04 ± 5.65	100.40 ± 16.10	0.37 ± 0.04*	693.81 ± 60.69**	6.65 ± 1.50	10.46 ± 0.77**
20 mg/kg	42.75 ± 5.52**	104.50 ± 28.89	0.41 ± 0.03*	717.33 ± 90.47**	6.75 ± 0.50	10.80 ± 0.92**

* A value significantly ($P < 0.05$) differed from the PBS group.
** A value significantly ($P < 0.01$) differed from the PBS group.

Table 4
Changes of hematology parameters of mice induced by NDs ($n = 10$).

Parameters	Value (mean ± SD) by exposure group				
	Control	PBS	0.8 mg/kg	4 mg/kg	20 mg/kg
Red blood cells ($\times 10^6/\mu L$)	7.65 ± 1.01	8.04 ± 0.303	7.61 ± 0.19	7.89 ± 0.335	7.53 ± 0.45
Hemoglobin (g/dl)	12.63 ± 0.34	13.33 ± 0.41	12.12 ± 0.36	12.83 ± 0.40	12.88 ± 0.42
Packed cell volume (%)	47.97 ± 0.84	49.18 ± 1.33	49.485 ± 1.07	49.15 ± 1.05	49.58 ± 0.88
Mean corpuscular volume (fl)	16.57 ± 0.31	16.58 ± 0.40	16.63 ± 0.26	16.25 ± 0.54	17.10 ± 0.50
Mean corpuscular hemoglobin (pg)	36.80 ± 5.42	39.53 ± 1.49	36.05 ± 2.51	38.78 ± 1.60	37.3 ± 1.94
Mean corpuscular Hemoglobin concentration (g/dl)	34.50 ± 0.87	33.73 ± 0.45	33.65 ± 0.63	33.08 ± 0.65	34.53 ± 0.78
Reticulocytes ($\times 10^3/\mu L$)	2.10 ± 0.44	2.17 ± 0.29	2.30 ± 0.28*	2.40 ± 0.42*	2.70 ± 0.28**
White blood cells ($\times 10^3/\mu L$)	4.08 ± 0.52	3.46 ± 0.16*	3.24 ± 0.51*	2.43 ± 0.50**	2.21 ± 0.51**
Percent of neutrophils (%)	45.57 ± 8.67	25.60 ± 1.99*	27.77 ± 3.70*	24.77 ± 3.71*	29.27 ± 2.31*
Band neutrophils ($\times 10^3/\mu L$)	0.00 ± 0.00	0.00 ± 0.00	0.00 ± 0.00	0.00 ± 0.00	0.00 ± 0.00
Percent of Lymphocytes ($\times 10^3/\mu L$)	49.47 ± 9.74	65.55 ± 6.68*	63.13 ± 7.83*	63.98 ± 9.34*	64.48 ± 8.10*
Monocytes ($\times 10^3/\mu L$)	0.10 ± 0.07	0.08 ± 0.08	0.08 ± 0.05	0.06 ± 0.07	0.07 ± 0.05
Eosinophils ($\times 10^3/\mu L$)	0.09 ± 0.07	0.11 ± 0.08	0.13 ± 0.08	0.09 ± 0.08	0.11 ± 0.06
Basophils ($\times 10^3/\mu L$)	0.01 ± 0.01	0.01 ± 0.01	0.01 ± 0.01	0.01 ± 0.01	0.01 ± 0.01
Platelets ($\times 10^3/\mu L$)	1074.33 ± 54.99	1165 ± 32.79	1225 ± 148.23*	1346.67 ± 112.88*	1536.50 ± 92.52*

* A value significantly ($P < 0.05$) differed from the PBS group.
** A value significantly ($P < 0.01$) differed from the PBS group.

dose-dependent increase in the experimental groups, suggesting an adverse influence of NDs on liver function.

Kidney function was also evaluated by analysis of the BUN and Cr values in serum. In this work, the levels of Cr did not show a significant difference ($P < 0.05$), whereas BUN showed significant differences between the experimental groups and the PBS control. These results indicate that NDs exposure also induces toxicological effects on the kidney and impairs function.

3.3.4. Complete blood cell counts

To assess the hematology biocompatibility of NDs with mice, all hematological parameters were measured (refer to Table 4). The hematological parameters, including erythrocytes, erythrocrit, mean corpuscular hemoglobin, mean corpuscular volume and hemoglobin, remained within the normal range in the experimental groups. However, in the experimental groups the values of platelet, reticulocytes and lympholeukocyte were slightly but significantly increased and the values of white blood cell and neutrophilic granulocyte were significantly decreased. The changes in hematological parameters indicate that significant inflammation was induced after exposure to NDs. These results are consistent with previous toxicological studies of other nanomaterials (Ji et al., 2007; Kim et al., 2006; Lewin et al., 2000).

4. Discussions

The radiotracer technique, with the advantages of high sensitivity, credibility, and freedom from interference, has become a unique approach to investigate the absorption, distribution, metabolism and excretion (ADME) of nanomaterials. This technique has been widely used to investigate the biodistribution of carbon nanomaterials in living systems, including carbon nanotubes (Guo et al., 2007; Liu et al., 2007b; Singh et al., 2006; Wang et al., 2004), C_{60} (Xu et al., 2007) and NDs (Yuan et al., 2009). The main feature of distribution obtained from radiotracer technique has been approved by a variety of imaging and spectroscopy techniques (Yang et al., 2007; Liu et al., 2007b). However, few reports exist thus far on the biodistribution of carbon nanoparticles administered by intratracheal instillation (Xu et al., 2007). The key issue that the tracer measurement technique can accurately represent the true biodistribution is the high stability of the radiolabeled nanomaterials. Re (V) has strong coordination capacity; which is easy to bind to some molecules and form stable coordination compounds. In the present work, the stannous chloride, as reducing agents, reduced Re (VII) into Re (V) possessing unfilled electron orbits in the reaction system. The unfilled electron orbits of Re (V) were filled by electrons donated by carboxyl and hydroxyl groups from NDs immediately. Thus the chelate complex, ^{188}Re-NDs, with good stability was formed. The

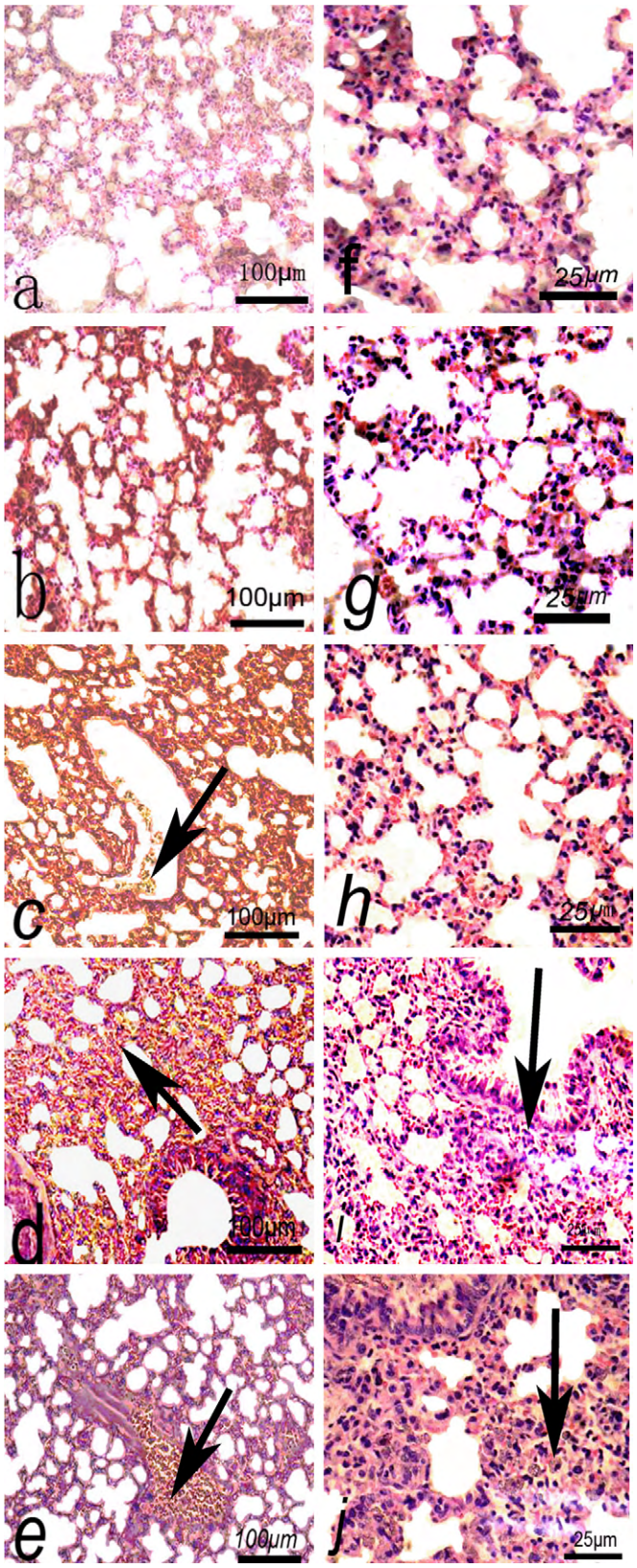

Fig. 2. Histopathology evaluation of lungs tissue in Kun Ming mouse after exposure to NDs by intratracheal instillation (a–e: magnification = 100× and f–j: magnification = 400×). (a and f) Control group, (b and g) PBS group, (c and h) 0.8 mg/kg group, (d and i) 4 mg/kg group, (e and j) 20 mg/kg group. Note the tissue accumulation of foamy alveolar macrophages within alveolar spaces, terminal bronchiolar alveolar junction (arrows in c–e). The accumulation of lipid filled macrophages, lacks of clearance, and development of tissue thickening are common features of the progressive nature of particle-induced lung disease (arrows in i and j).

experimental determination of radiochemical purity indicated that approximately 80% of the labeled compound remained intact in mouse serum at 4 h post-intratracheal instillation. Therefore, the distribution of ^{188}Re obtained in this work could accurately reflect the biodistribution of NDs in living mice.

As mentioned previously, most of the ^{188}Re-NDs accumulated in lung and the % ID/g values of lung uptake reached as high as 190% within 4 h after intratracheal instillation. Considering the average lung weight of mice (0.33 g), the fraction of ^{188}Re-NDs retained in the lung amounted to 63.4% of the total dose instilled. The high lung uptake was verified by microscopic images of pathological sections. As can be seen from Fig. 2c–e, there were many granules formed from aggregation of NDs in the terminal bronchiolar alveolar junction of lung sections, but not in liver, spleen, and kidney (data not shown). The observations of histological sections with optical microscopy gave additional support for the distribution validity of NDs obtained by tracer techniques.

We also found that the clearance of ^{188}Re-NDs from the lung was slow, although a part of the radioactivity decreased from lung was possibly due to Re released from Re-NDs. The % ID/g values of the lung were maintained at 90.72% and 69.06% (or 33.5% and 26.85% of total dose instilled) at 24 h and 48 h, respectively.

It has been reported that after intratracheal instillation with $Na^{99m}TcO_4$, most of these comparatively smaller molecules were transported to the circulation system through the air–blood barrier, and then quickly cleared with the urine, with no obvious retention in the lung and other organs (Xu et al., 2007). In a separate experiment, we also observed the distribution characteristic of $Na^{188}ReO_4$ is quite different from that of ^{188}Re-NDs (data not shown). Therefore, the overall features of the biodistribution characterized in this work, such as high lung uptake, slow lung clearance, and low urine excretion, provide additional support for the reliability of a biodistribution assessment based on stable ^{188}Re-NDs.

The biodistribution of NDs in mice measured by the radiotracer technique provides guidance for the examination and understanding of respiratory toxicity after intratracheal instillation. Due to the highest uptake and long retention time of NDs in lung tissue, the lung suffered the most severe toxicological effects and damage. Lung tissue thickening, lung inflammatory responses, as well as changes in the biochemical parameters of BAL fluids demonstrated this significant pulmonary toxicity. The experiments with radiotracers also indicate that the NDs instilled into lung had the ability to penetrate the alveolar-capillary barrier into blood circulation. The NDs circulating in blood were easy to be immunologically recognized and caught by the reticuloendothelial system, and then accumulated in liver, bone, and spleen. As such, systematic toxicity of NDs after intratracheal instillation also occurred, as evidenced typically by a dose-dependent adverse influence on liver and kidney function, as well as blood cells. Previous studies have indicated that NDs are biocompatible with various cell types, with no noticeable cytotoxicity found in *in vitro* tests (Liu et al., 2007a; Schrand et al., 2007a; Yu et al., 2005). In this work, however, we found that NDs induced not only a significant pulmonary toxicity, but also a dose-dependent systemic toxicity after NDs intratracheal instillation. As respiratory inhalation is one of the most possible exposure routes, the data on lung and systemic toxicity obtained from this work may be very crucial for the examination and assessment of NDs biosafety.

In a previous work, the biodistribution of a polyhydroxylated derivative of fullerene $C_{60}(OH)_x$ (x = 22–24) was studied in Sprague–Dawley rats after intratracheal instillation (Xu et al., 2007). The *in vivo* behavior of NDs observed in the present work was found to be very similar to that of $C_{60}(OH)_x$ labeled with ^{99m}Tc. However, it is worth noting the slight differences in biodistribution and particle fate between $C_{60}(OH)_x$ and NDs. In view of the long-term retention in the lung and the very fast clearance from

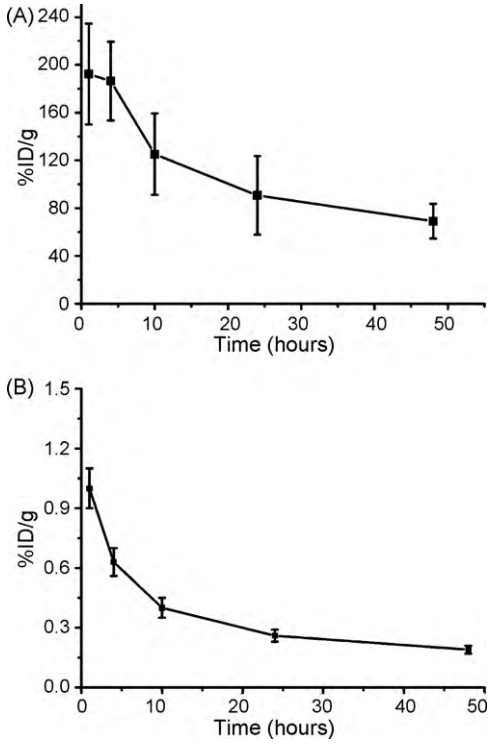

Fig. 3. Clearance curves of lung (A) and blood (B).

the blood, Xu et al. proposed a transient characteristic of penetrating the alveolar-capillary barrier for $C_{60}(OH)_x$. However, this work demonstrated that the clearance of NDs from the blood and lung was almost synchronous, as shown in Fig. 3. The similar clearance speed rate implies that the NDs retained in the lung could continuously penetrate the alveolar-capillary barrier, and diffuse into the blood circulation, thus supplying the depletion of NDs in the blood circulation process. Accordingly, it seems to indicate that NDs were more capable of penetrating the biological barrier than fullerene derivatives. In a separate *in vitro* experiment, we also found that NDs labeled with ^{188}Re could easily be internalized into Hela cells, and the uptake rate of NDs was twice as high as that of multi-walled carbon nanotubes. The results from the *in vitro* study give additional support for the enhanced capability of penetrating biological barriers. Thus, more attention should be paid to the injury of various critical organs, including the heart and brain when carried out a toxicity examination and assessment of NDs. As indicated in Table 1, the uptake of NDs in the heart was obviously high, and was even higher than the uptake level observed in liver and blood. It is reasonable to speculate that respiratory exposure to NDs may be closely associated with cardiovascular adverse effects. The adverse influence of ambient ultrafine particles (Brook et al., 2004) and single-walled carbon nanotubes (Li et al., 2007b) on the cardiovascular system has been confirmed. Due to the unique property of NDs that has emerged from this work, the future study of respiratory toxicity of NDs to the cardiovascular system is of considerable interest.

5. Conclusions

The biodistribution and acute toxicity of NDs in mice after intratracheal instillation was investigated by the radiotracer technique and a series of biological assays. Results indicated that NDs could penetrate the air–blood barrier into the circulation system and redistribute to the spleen, liver, and bone. Approximately 63.4% of the total instilled NDs accumulated in the mouse lung within 4 h post-instillation, and was maintained at a high level for over 48 h. This long-term retention of NDs induced significant toxicity in lung in the 4 mg/kg and 20 mg/kg experimental groups. The dose-dependent liver and hematological toxicity was also observed at 3 days post-exposure. Although NDs are biocompatible with various cell types, the significant lung and systemic toxicity of NDs after intratracheal instillation suggested that much more attention should be paid to the toxicity of NDs. In this work, only the short-term toxicological response of NDs to mice was investigated. Further toxicological studies on chronic respiration toxicity to major target organs are required.

Conflict of interest

We declare that we have no financial and personal relationships with other people or organizations that can inappropriately influence our work, there is no professional or other personal interest of any nature or kind in any product, service and/or company that could be construed as influencing the position presented in, or the review of, the manuscript entitled.

Acknowledgements

We wish to thank Yan Peng from Gansu Gold Stone Nano.Material Co., Ltd. generously supplied the NDs. This work was supported by the National Science Foundation of China (Nos. 10905086, 10975179), the Shanghai Municipal Natural Science Foundation (Nos. 08ZR1422700, 08JC1422600), the Ministry of Health (No. 2009ZX10004-301), the CAS Innovation Program, and the MOST973 Program (No. 2006CB705605).

References

Bottini, M., Bruckner, S., Nika, K., Bottini, N., Bellucci, S., Magrini, A., Bergamaschi, A., Mustelin, T., 2006. Multi-walled carbon nanotubes induce T lymphocyte apoptosis. Toxicol. Lett. 160, 121–126.

Boudou, J.P., Curmi, P.A., Jelezko, F., Wrachtrup, J., Aubert, P., Sennour, M., Balasubramanian, G., Reuter, R., Thorel, A., Gaffet, E., 2009. High yield fabrication of fluorescent NDs. Nanotechnology 20, 235602.

Brook, R.D., Franklin, B., Cascio, W., Hong, Y., Howard, G., Lipsett, M., Luepker, R., Mittleman, M., Samet, J., Smith Jr., S.C., 2004. Air pollution and cardiovascular disease: a statement for healthcare professionals from the Expert Panel on Population and Prevention Science of the American Heart Association. Circulation 109, 2655–2671.

Chao, J.I., Perevedentseva, E., Chung, P.H., Liu, K.K., Cheng, C.Y., Chang, C.C., Cheng, C.L., 2007. Nanometer-sized diamond particle as a probe for biolabeling. Biophys. J. 93, 2199–2208.

Chen, M., Pierstorff, E.D., Lam, R., Li, S.Y., Huang, H., Osawa, E., Ho, D., 2009. Nanodiamond-mediated delivery of water-insoluble therapeutics. ACS Nano 3, 820–827.

Donaldson, K., Aitken, R., Tran, L., Stone, V., Duffin, R., Forrest, G., Alexander, A., 2006. Carbon nanotubes: a review of their properties in relation to pulmonary toxicology and workplace safety. Toxicol. Sci. 92, 5–22.

Fu, C.C., Lee, H.Y., Chen, K., Lim, T.S., Wu, H.Y., Lin, P.K., Wei, P.K., Tsao, P.H., Chang, H.C., Fann, W., 2007. Characterization and application of single fluorescent NDs as cellular biomarkers. Proc. Natl. Acad. Sci. U.S.A. 104, 727–732.

Guo, J., Zhang, X., Li, Q., Li, W., 2007. Biodistribution of functionalized multiwall carbon nanotubes in mice. Nucl. Med. Biol. 34, 579–583.

Huang, H., Pierstorff, E., Osawa, E., Ho, D., 2007. Active nanodiamond hydrogels for chemotherapeutic delivery. Nano Lett. 7, 3305–3314.

Huang, H., Pierstorff, E., Osawa, E., Ho, D., 2008. Protein-mediated assembly of nanodiamond hydrogels into a biocompatible and biofunctional multilayer nanofilm. ACS Nano 2, 203–212.

Ji, J.H., Jung, J.H., Kim, S.S., Yoon, J.U., Park, J.D., Choi, B.S., Chung, Y.H., Kwon, I.H., Jeong, J., Han, B.S., 2007. Twenty-eight-day inhalation toxicity study of silver nanoparticles in Sprague–Dawley rats. Inhal. Toxicol. 19, 857–871.

Kim, J.S., Yoon, T.J., Yu, K.N., Kim, B.G., Park, S.J., Kim, H.W., Lee, K.H., Park, S.B., Lee, J.K., Cho, M.H., 2006. Toxicity and tissue distribution of magnetic nanoparticles in mice. Toxicol. Sci. 89, 338–347.

Lam, C., James, J.T., McCluskey, R., Arepalli, S., Hunter, R.L., 2006. A review of carbon nanotube toxicity and assessment of potential occupational and environmental health risks. Crit. Rev. Toxicol. 36, 189–217.

Lewin, M., Carlesso, N., Tung, C.H., Tang, X.W., Cory, D., Scadden, D.T., Weissleder, R., 2000. Tat peptide-derivatized magnetic nanoparticles allow *in vivo* tracking and recovery of progenitor cells. Nat. Biotechnol. 18, 410–414.

Li, J.G., Li, W.X., Xu, J.Y., Cai, X.Q., Liu, R.L., Li, Y.J., Zhao, Q.F., Li, Q.N., 2007a. Comparative study of pathological lesions induced by multiwalled carbon nanotubes in lungs of mice by intratracheal instillation and inhalation. Environ. Toxicol. 22, 415–422.

Li, Z., Hulderman, T., Salmen, R., Chapman, R., Leonard, S.S., Young, S.H., Shvedova, A., Luster, M.I., Simeonova, P.P., 2007b. Cardiovascular effects of pulmonary exposure to single-wall carbon nanotubes. Environ. Health Perspect. 115, 377–382.

Liu, K.K., Cheng, C.L., Chang, C.C., Chao, J.I., 2007a. Biocompatible and detectable carboxylated nanodiamond on human cell. Nanotechnology 18, 325102.

Liu, Z., Cai, W., He, L., Nakayama, N., Chen, K., Sun, X., Chen, X., Dai, H., 2007b. *In vivo* biodistribution and highly efficient tumour targeting of carbon nanotubes in mice. Nat. Nanotechnol. 2, 47–52.

Magrez, A., Kasas, S., Salicio, V., Pasquier, N., Seo, J.W., Celio, M., Catsicas, S., Schwaller, B., Forro, L., 2006. Cellular toxicity of carbon-based nanomaterials. Nano Lett. 6, 1121–1125.

Puzyr, A.P., Baron, A.V., Purtov, K.V., Bortnikov, E.V., Skobelev, N.N., Mogilnaya, O.A., Bondar, V.S., 2007. NDs with novel properties: a biological study. Diam. Relat. Mater. 16, 2124–2128.

Schrand, A.M., Dai, L., Schlager, J.J., Hussain, S.M., Osawa, E., 2007a. Differential biocompatibility of carbon nanotubes and NDs. Diam. Relat. Mater. 16, 2118–2123.

Schrand, A.M., Huang, H., Carlson, C., Schlager, J.J., Sawa, E., Hussain, S.M., Dai, L., 2007b. Are diamond nanoparticles cytotoxic? J. Phys. Chem. B 111, 2–7.

Singh, R., Pantarotto, D., Lacerda, L., Pastorin, G., Klumpp, C., Prato, M., Bianco, A., Kostarelos, K., 2006. Tissue biodistribution and blood clearance rates of intravenously administered carbon nanotube radiotracers. Proc. Natl. Acad. Sci. U.S.A. 103, 3357–3362.

Sun, Y.P., Fu, K., Lin, Y., Huang, W., 2002. Functionalized carbon nanotubes: properties and applications. Acc. Chem. Res. 35, 1096–1104.

Thostenson, E.T., Ren, Z., Chou, T.W., 2001. Advances in the science and technology of carbon nanotubes and their composites: a review. Compos. Sci. Technol. 61, 1899–1912.

Ueng, T.H., Kang, J.J., Wang, H.W., Cheng, Y.W., Chiang, L.Y., 1997. Suppression of microsomal cytochrome P450-dependent monooxygenases and mitochondrial oxidative phosphorylation by fullerenol, a polyhydroxylated fullerene C_{60}. Toxicol. Lett. 93, 29–37.

Wang, H., Wang, J., Deng, X., Sun, H., Shi, Z., Gu, Z., Liu, Y., Zhao, Y., 2004. Biodistribution of carbon single-wall carbon nanotubes in mice. J. Nanosci. Nanotechnol. 4, 1019.

Xu, J.Y., Li, Q.N., Li, J.G., Ran, T.C., Wu, S.W., Song, W.M., Chen, S.L., Li, W.X., 2007. Biodistribution of ^{99m}Tc-$C_{60}(OH)_x$ in Sprague–Dawley rats after intratracheal instillation. Carbon 45, 1865–1870.

Yang, S., Guo, W., Lin, Y., Deng, X., Wang, H., Sun, H., Liu, Y., Wang, X., Wang, W., Chen, M., 2007. Biodistribution of pristine single-walled carbon nanotubes in vivo. J. Phys. Chem. C 111, 17761–17764.

Yu, S.J., Kang, M.W., Chang, H.C., Chen, K.M., Yu, Y.C., 2005. Bright fluorescent NDs: no photobleaching and low cytotoxicity. J. Am. Chem. Soc. 127, 17604–17605.

Yuan, Y., Chen, Y., Liu, J.H., Wang, H., Liu, Y.F., 2009. Biodistribution and fate of NDs *in vivo*. Diam. Relat. Mater. 18, 95–100.